$$\sum_{m=2}^{N}\sum_{a_m} p(a|b)\,\delta(b,a_m)\ln(y+s_m^{m-1})P_m =$$

$$\sum_{m=2}^{N}\sum_{a_{m-1}} p(a|b)p(b|a_{m-1})\ln(y+s_b^{m-1})\,P_1(a_{m-1}) =$$

$$(N-1)\sum_{c} p(a|b)\,p(b|c)\ln(y+s_b^c)\,P_1(c)$$

The second term is

$$\sum_{m=2}^{N}\sum_{a_m} p(a|b)\,\delta(b,a_m)\ln(L_m^{m-1}y+W_m)P_m =$$

$$p(a|b)\sum_{m=2}^{N}\sum_{c}\sum_{a_{m-1}} p(b|c)\,\delta(c,a_{m-1})\ln(L_b^c y+W_{m-1})P_{m-1} =$$

$$p(a|b)\sum_{m=1}^{N-1}\sum_{c}\sum_{a_m} p(b|c)\,\delta(c,a_m)\ln(L_b^c y+W_m)P_m =$$

$$(N-1)p(a|b)\sum_{c} C_{N-1}(y,b,c)$$

The third term can be written in the same way as the second term. Finally, from the definition, the last term is simply

$$\sum_{a_1} p(a|b)\,\delta(b,a_1)\ln(y+W_1)\,P_1(a_1) = C_1(y,a,b)$$

Equation 19 is obtained by letting $N = 1$ in eq 11, viz.

$$C_1(y,a,b) = \sum_{a_1}\ln(y+W_1)\,p(a|b)\,\delta(b,a)\,P_1(b)$$

$$= \ln(y+W_1)\,p(a|b)\,P_1(b)$$

Since $W_1 = s_1^0\sigma_1^0$ and $p(a|b)\,P_1(b) = P_2(a,b)$, eq 19 results.

## References and Notes


(1) von Dreele, P. H.; Poland, D.; Scheraga, H. A. *Macromolecules* **1971**, *4*, 396.
(2) Wójcik, J.; Altmann, K. H.; Scheraga, H. A. *Biopolymers*, in press.
(3) Zimm, B. H.; Bragg, J. K. *J. Chem. Phys.* **1959**, *31*, 526.
(4) Scheraga, H. A. *Pure Appl. Chem.* **1973**, *36*, 1; **1978**, *50*, 315.
(5) Kidera, A.; Mochizuki, M.; Hasegawa, R.; Hayashi, T.; Sato, H.; Nakajima, A.; Fredrickson, R. A.; Powers, S. P.; Lee, S.; Scheraga, H. A. *Macromolecules* **1983**, *16*, 162.
(6) Miki, T.; Kidera, A.; Oka, M.; Hayashi, T.; Nakajima, A.; Meinwald, Y. C.; Thannhauser, T. W.; Scheraga, H. A. *Macromolecules* **1985**, *18*, 1069.
(7) Ananthanarayanan, V. S.; Andreatta, R. H.; Poland, D.; Scheraga, H. A. *Macromolecules* **1971**, *4*, 417.
(8) Platzer, K. E. B.; Ananthanarayanan, V. S.; Andreatta, R. H.; Scheraga, H. A. *Macromolecules* **1972**, *5*, 177.
(9) Van Wart, H. E.; Taylor, G. T.; Scheraga, H. A. *Macromolecules* **1973**, *6*, 266.
(10) Dygert, M. K.; Taylor, G. T.; Cardinaux, F.; Scheraga, H. A. *Macromolecules* **1976**, *9*, 794.
(11) Scheule, R. K.; Cardinaux, F.; Taylor, G. T.; Scheraga, H. A. *Macromolecules* **1976**, *9*, 23.
(12) Fujita, H.; Teramoto, A.; Yamashita, T.; Okita, K.; Ikeda, S. *Biopolymers* **1966**, *4*, 781.
(13) Ferger, M. F.; Jones, W. C.; Dyckes, D. F.; Du Vigneaud, V. *J. Am. Chem. Soc.* **1977**, *94*, 982.
(14) von Dreele, P. H.; Lotan, N.; Ananthanarayanan, V. S.; Andreatta, R. H.; Poland, D.; Scheraga, H. A. *Macromolecules* **1971**, *4*, 408.
(15) Leach, S. J.; Scheraga, H. A. *J. Am. Chem. Soc.* **1960**, *82*, 4790.
(16) Lang, C. A. *Anal. Chem.* **1958**, *30*, 1692.
(17) Noel, R. J.; Hambleton, L. G. *J. Assoc. Off. Anal. Chem.* **1976**, *59*, 134; *Chem. Abstr.* **1976**, *84*, 149347.
(18) Chervenka, C. H. *A Manual of Methods for the Analytical Ultracentrifuge*; Beckman Instruments: Palo Alto, CA, 1969; pp 47-49.
(19) Moffitt, W.; Yang, J. T. *Proc. Natl. Acad. Sci. U.S.A.* **1956**, *42*, 596.
(20) Urnes, P. J.; Doty, P. *Adv. Protein Chem.* **1961**, *16*, 401.
(21) Lehman, G. W.; McTague, J. P. *J. Chem. Phys.* **1968**, *49*, 3170.
(22) Greenfield, N.; Fasman, G. D. *Biochemistry* **1969**, *8*, 4108.
(23) Scheraga, H. A. *Proc. Natl. Acad. Sci. U.S.A.* **1985**, *82*, 5585.
(24) Vásquez, M.; Scheraga, H. A. *Biopolymers* **1988**, *27*, 41.
(25) Only a small improvement was obtained in the optimization when eight different values of $\Delta H$ and $\Delta S$ were used for the four specific interactions; the value of the target function was 0.070.
(26) Poland, D.; Scheraga, H. A. *Biopolymers* **1965**, *3*, 283.


# A Reptation Model for Polymer Dissolution


**Michael F. Herman* and S. F. Edwards**

*Cavendish Laboratory, Madingley Road, Cambridge CB3 0HE, U.K.*



*Received May 15, 1989; Revised Manuscript Received January 30, 1990*



ABSTRACT: A model for the dissolution of a simple linear polymer in a solvent is presented. When the pure polymer and solvent are brought into contact, the solvent penetrates the polymer, causing it to swell. This swelling induces a nonrandom distribution of orientations for the polymer chains. The contribution to the free energy and chemical potentials of polymer and solvent due to this nonrandom distribution of orientations is evaluated in closed form from reptation theory. When this contribution is sufficiently large compared with the ordinary mixing terms, the system undergoes a phase separation into a gel-like concentrated solution phase and a dilute solution phase. The presence of this gel-like phase can significantly slow the dissolution process. Simple model calculations are present to illustrate the expected behavior of solvent/polymer systems for which the magnitude of the orientational contribution to the free energy is sufficiently large to support a phase boundary between concentrated and dilute solution regions.


## I. Introduction

The dissolution of a polymer in a solvent is a process of considerable technological importance. If a specific polymer has a desirable property in solution but the kinetics of dissolution are prohibitively slow, then the slow rate of dissolution may limit its usefulness. By understanding the dissolution process and the underlying physical parameters that affect the nature and rate of this process, it may be possible to alter the polymer/solvent


* Permanent address: Department of Chemistry and the Quantum Theory Group, Tulane University, New Orleans, LA 70118.



0024-9297/90/2223-3662$02.50/0

system in ways which improve the dissolution rate without adversely affecting the desired properties of the system.

In a previous paper considering these questions, Brochard and de Gennes[1] discuss how the swelling of the polymer due to the influx of solvent results in an elastic-like stress opposing the solvent influx. They predict that a gel-like swollen polymer state can form. The subsequent dissolution of the polymer from this swollen state is governed by the rate of the relaxation of the stress. This rate should be on the order of the reptation disengagement time,[2] $\tau_d$. They call this stress relaxation and dissolution of the swollen polymer state the viscous yield phase of the dissolution process. In this paper we consider in detail the stress accompanying the swelling of the polymer within the reptation model.[2] More specifically, we evaluate contributions to the solvent and polymer chemical potentials due to the deformation of the polymer system as it swells. The swelling induces a nonrandom distribution of orientations for the segments in the primitive chain, which describes the dynamics of the polymer in the reptation model. This nonrandom distribution is evaluated as a function of the dilution of the polymer system. The contribution to the free energy per unit volume due to this orientational distribution is obtained in closed form, and from this the chemical potentials are evaluated. We find that the form of the chemical potentials does support a gel-like swollen phase if the magnitude of the orientational contribution is great enough compared with the ordinary mixing terms in the free energy and chemical potentials. This gel-like solution phase coexists with a dilute solution phase. An essentially pure polymer region also exists along with these two solution phases at early times. We analyze the manner in which some of the microscopic physical features of the polymer affect the relative magnitudes of the mixing and orientational contributions. The presence of this gel-like phase can significantly slow the dissolution process. Wnen it is not present, stirring of the solution avoids buildup of polymer at the interphase with the pure polymer, hastening the dissolution process. When a gel-like phase is present, then the dissolution of pure polymer is slowed until the stress has relaxed sufficiently to dissolve this concentrated solution. This is controlled by the reptation disengagement time, as pointed out by Brochard and de Gennes.[1]

We construct the differential equations that govern the kinetics of this viscous yield process and suggest simplifying approximations that should be applicable for these systems. These equations require a model for the concentration dependence of the disengagement time. In general, this dependence is not well understood at the present time.

In section II we evaluate the contribution to the free energy and chemical potentials arising from the deformation of the entangled polymer system due to the swelling. The parameters affecting the relative magnitudes of the various contributions are analyzed. The equations governing the relaxation of the orientational contributions to the chemical potentials are considered. In section III model calculations are presented to illustrate the time evolution of the concentrated solution/dilute solution system.

## II. Theory

**A. Free Energy and Chemical Potential.** Let $\bar{G}(\phi_p,T,P)$ be the free energy per volume as a function of $T$, $P$, and the polymer volume fraction, $\phi_p$. The free energy of a small region of volume $V$ is $G = \bar{G}V$, where we take $\phi_p$ to be constant over this small region. The solvent chemical potential is defined by

$$\mu_s = \left(\frac{\partial G}{\partial n_s}\right)_{n_p} = \bar{G}\left(\frac{\partial V}{\partial n_s}\right)_{n_p} + V\left(\frac{\partial \phi_p}{\partial n_s}\right)_{n_p}\frac{\partial \bar{G}}{\partial \phi_p} \quad (1)$$

where all derivatives are evaluated at constant $T$ and $P$. The volume is given by

$$V = n_s V_s + n_p V_p \quad (2)$$

where $n_s$ and $n_p$ are the number of solvent molecules and the number of polymer chains in the region, respectively. $V_p$ is the average volume per polymer chain, and $V_s$ is the average volume per solvent molecule. $V_p$ and $V_s$ are assumed independent of $\phi_p$ throughout this work. The polymer volume fraction is given by $\phi_p = n_p V_p/V$. Therefore, $\mu_s$ is obtained as

$$\mu_s = -V_s\phi_p^2\frac{\partial}{\partial \phi_p}(\bar{G}/\phi_p) \quad (3)$$

Similar argument yields

$$\mu_p = \left(\frac{\partial G}{\partial n_p}\right)_{n_s} = \bar{G}\left(\frac{\partial V}{\partial n_p}\right)_{n_s} + V\left(\frac{\partial \phi_p}{\partial n_p}\right)_{n_s}\frac{\partial \bar{G}}{\partial \phi_p}$$

$$= V_p\left[\bar{G} + (1-\phi_p)\frac{\partial \bar{G}}{\partial \phi_p}\right] \quad (4)$$

There are two free energy contributions that we include in our model. The first is the usual contribution arising from spatial variations in the concentration. This produces a term in the solvent chemical potential that is proportional to the osmotic pressure[3] $\Pi$

$$\mu_s^{OP} = -V_s\Pi \quad (5)$$

where the superscript OP refers to osmotic pressure. Given a functional form for $\Pi$, $\bar{G}^{OP}$ can be obtained from (3) (up to an unimportant constant of integration), which in turn provides $\mu_p^{OP}$.

The second term accounts for the stress that arises from the deformation of the entangled polymer system due to the influx of solvent. We employ the reptation model[2] of polymer dynamics in order to calculate this free energy contribution. The reptation model assumes that the entanglements felt by a given polymer chain due to the presence of other polymer chains can be treated by surrounding the polymer by a tube. The polymer slithers along this tube in a curvillinear one-dimensional diffusive motion.

The curve running along the center of the tube is called the primitive path. The polymer chain is replaced by a one-dimensional primitive chain that executes Rouse-like motion along the primitive path. The average length, $a(\phi_p)$, of each segment in this equivalent chain is identified with the distance between entangements, and it depends on $\phi_p$. The number of segments in the primitive chain, $Z(\phi_p)$, is determined by the requirements that the mean squared end-to-end distance of the primitive chain is the same as that for the original chain. The average contour length of the primitive chain is $L(\phi_p) = Za$.

As the solvent is drawn into the polymer network, the network swells. This swelling stretches the network in one direction. For instance, if the polymer is on the bottom of a reaction vessel and solvent is added on top of it, the swelling must occur in the upward direction. If the

polymer is in spherical particles immersed in solvent, then the swelling is radial. The swelling stretches the reptation tube, changing its length and also the orientation of each segment of the primitive chain. As the tube length changes, the contour length of the primitive chain tends to stretch as the entanglements drag the chain segments along. This competes with relaxation or contraction of the chain within the tube, which is governed by the Rouse modes of the primitive chain. We are primarily interested in the case where the swelling of the network takes place on a macroscopic time scale. On this time scale, the Rouse relaxation of the contour length is generally very rapid. Consequently, the primitive chain modes can be taken to be fully relaxed, and the average contour length of this chain can be treated as constant. An exception to this time scale separation may occur as the solvent begins to penetrate an essentially pure glassy polymer. Because of the glassy nature of the pure polymer, the relaxation of contour length is comparatively slow and may occur on the same time scale as the swelling. However, even in this case the contour length relaxation is rapid compared with swelling in all regions that have a significant amount of solvent present. An additional free energy contribution to account for the chain stretching is required only for a narrow range of solvent concentrations near the pure polymer limit. We return to this point in terms of simple model calculations in section III. Here we do not worry about this complication and consider the contour length relaxation to be very fast on the time scale of the swelling. Given this assumption there is no free energy contribution due to elastic stretching of the chain as the network swells. This differs from the case of a true cross-linked gel where the elastic stretching contribution is of central importance. However, in our system there is still a free energy contribution due to the reorientation of the primitive chain segments which accompanies the swelling. Below we consider the effect of stress relaxation, but first we discuss the contribution to the free energy and chemical potentials in the absence of stress relaxation.

Suppose at time $t_0$ a chain segment has a random distribution of orientations. Let $\phi_{p0}$ be the polymer volume fraction at the position of this chain segment. At some time later, $t_1$, the polymer volume fraction is reduced to $\phi_{p1}$ due to the influx of solvent. In Appendix A we evaluate the distribution of orientations for the chain segment at $t_1$. This distribution $f(\cos\theta;\Phi)$ depends only on $\theta$, the angle between the direction of the swelling and the orientation of the chain segment, and on $\Phi = \phi_{p1}/\phi_{p0}$, which determines the extent of the local swelling of the polymer/solvent system. Given this distribution, the orientational contribution to the free energy from this chain segment is given by

$$\Delta G_{seg}^{OR}(\Phi) = -T\Delta S_{seg}(\Phi) = K_B T \int_{-1}^{1} d\xi\, [f(\xi;\Phi) \ln f(\xi;\Phi) - f_0 \ln f_0] \quad (6)$$

where $\xi = \cos\theta$, $f_0 = {}^1/_2$ is the original random distribution, $T$ is the temperature in Kelvins, and $K_B$ is Boltzmann's constant. Substitution of (A6) for $f(\xi;\Phi)$ and evaluation of the $\xi$ integral lead to

$$\Delta G_{seg}^{OR} = K_B T\left[-2\ln\Phi - 3 + \frac{3\Phi\cos^{-1}\Phi}{\sqrt{1-\Phi^2}}\right] \quad (7)$$

The free energy change per chain $\Delta G_{chain}$ for this dilution-swelling process is obtained by multiplying $\Delta G_{seg}^{OR}$ by the number of segments $Z(\phi_p)$. In order to get the contribution to the free energy per unit volume, we simply multiply $\Delta G_{chain}$ by the number of chains per unit volume, which is given by $n_p/V = \phi_p/V_p$. Therefore

$$\bar{\Delta}\bar{G}^{OR} = \frac{Z\phi_p}{V_p}\Delta G_{seg}^{OR} \quad (8)$$

The corresponding orientational contributions to $\mu_s$ and $\mu_p$ can be obtained from (3) and (4). When evaluating $\mu_s^{OR}$ and $\mu_p^{OR}$, the $\phi_p$ dependence of $Z$ contributes to $\partial\Delta G/\partial\phi_p$. If this $\phi_p$ dependence is ignored, then the result obtained for $\mu_s$ in this way agrees with that obtained from the stress as calculated in the independent alignment approximation.[2]

At this point we focus on the solvent chemical potential. Since $\mu_s^{OP}$ is given by $-V_s\Pi$, it must be a monotonically decreasing function of the polymer volume fraction $\phi_p$. For small $\phi_p$, $\mu_s^{OP}$ is proportional to $-\phi_p$, and it scales as $\phi_p^{9/5}$ in the semidilute regime. A Flory–Huggins expression[3] for $\Delta G^{OP}$ should be qualitatively reasonable at high polymer concentrations, giving a $\mu_s^{OP} \to K_B T \ln(1-\phi_p)$ divergence as $\phi_p \to 1$. The orientational contribution is somewhat more complicated. Substitution of (8) into (3) yields

$$\mu_s^{OR} = \frac{-V_s}{V_p}\phi_p^2\left[\frac{dZ}{d\phi_p}\Delta G_{seg}^{OR} + Z\frac{\partial}{\partial\phi_p}\Delta G_{seg}^{OR}\right] \quad (9)$$

The number of primitive path segments $Z(\phi_p)$ is a monotonically increasing function of $\phi_p$, and it is proportional to the degree of polymerization $N$. Prior to the swelling of the polymer network, $\mu_s^{OR}$ is zero. As the polymer network swells (i.e., as $\phi_p$ decreases from unity), the orientational stress opposes the osmotic contribution, resisting further influx of solvent. As $\phi_p$ decreases, the contribution to the free energy per chain segment continues to increase. However, the distance between entanglements and the tube diameter increase, and the number of primitive path segments per chain and the number of chains per unit volume decrease. These factors tend to reduce the stress and the orientational contribution to the chemical potential. The interplay between the increasing stress per segment and the fewer segments per volume as $\phi_p$ decreases leads to the maximum in $\mu_s^{OR}$. As $\phi_p \to 0$, the chains are no longer entangled and the stress contribution vanishes.

The interplay between the osmotic pressure and orientational stress terms can lead to various types of behavior in $\mu_s$. Three cases are shown in Figure 1. In Figure 1, the explicit functional form

$$\mu_s^{OP} = -V_s\Pi = -\frac{K_B T V_s}{V_p}\phi_p\left[1 + \frac{7}{8}a_{OP}\phi_p(1 + 2a_{OP}\phi_p)^{1/4}\right] \quad (10)$$

is employed. This form is taken from the good-solvent limit of renormalization group treatment of the osmotic pressure of Cherayil et al.[4] for the case of linear polymers. The constant $a_{OP}$ is given by $A_2/V_p$, where $A_2$ is the second osmotic virial coefficient. Equation 10 is valid for dilute and semidilute solutions. In concentrated solutions,[3] $\mu_s^{OP}$ should behave as $K_B T \ln(1-\phi_p)$. However, as we shall see below, this deficiency in (10) as $\phi_p \to 1$ will have no effect on our qualitative conclusions. Following Cherayil et al.,[4] we can express $a_{OP}$ as

$$a_{OP} = A_2/V_p = 4\pi^{3/2}\Psi R_G^3/V_p \quad (11)$$

where $R_G$ is the radius of gyration and $\Psi$ is the penetration factor. Estimates of $\Psi$ for linear polymers range from 0.22 to 0.30.[4] We use 0.26 in our work. Suppose we take $R_G = bN^{3/5}/6^{1/2}$, where $b$ is on the order of the Kuhn length. This expression for $R_G$ is appropriate for dilute and se-

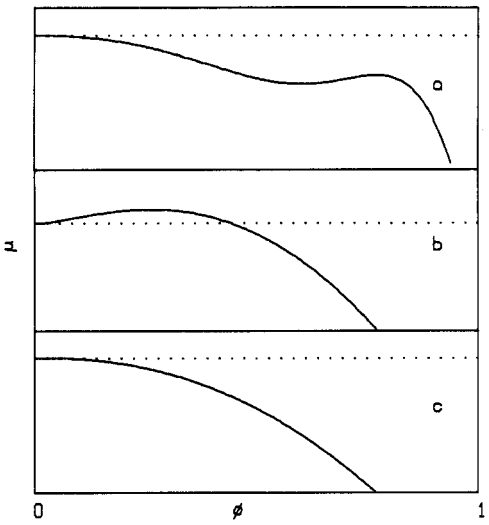


**Figure 1.** Solvent chemical potential is plotted vs polymer volume fraction. The functional form employed for the chemical potential is described in the text. The parameters used are $m = 8.0$, $Z_1 = 0.1$, and $B = 0.064$ for case a; $m = 1.0$, $Z_1 = 0.05$, and $B = 0.26$ for case b; and $m = 1.0$, $Z_1 = 0.01$, and $B = 2.6$ for case c. The degree of polymerization is 10 000 in each case. The dotted line specifies the zero of the chemical potential. The scale of the chemical potential axis is determined by the choice of the overall multiplicative constant $K_BTV_s/V_p$, which is left unspecified.

midilute solutions in the good-solvent limit, which is consistent with the expression used for the osmotic pressure. Since $V_p = V_mN$, where $V_m$ is the average monomer volume, $a_{OP}$ behaves as

$$a_{OP} = (0.39)BN^{4/5} \tag{12}$$

where $B \equiv b^3/V_m$. $B$ is taken to be independent of $\phi_p$, but it does depend on the specific polymer/solvent system investigated.

The qualitative behavior $\mu_s$ is determined by the relative values of $\mu_s^{OP}$ and $\mu_s^{OR}$. It is not affected by the value of the factor $V_sK_BT/V_p$ which multiplies both $\mu_s^{OP}$ and $\mu_s^{OR}$. The remaining unspecified factor is $Z(\phi_p)$, the number of segments in the primitive chain. In general, this function is an increasing function of polymer volume fraction, it vanishes as $\phi_p \to 0$, and it is proportional to $N$. We use the simple scaling form $Z = Z_1\phi^mN$, where $Z_1$ is independent of $N$. This form has the value $Z_1N$ for the melt. The value of $m$ determines how rapidly $Z$ decreases with increasing solvent volume fraction. Given these forms for $\Pi$ and $Z$, there are three parameters in the model for the total solvent chemical potential, $Z_1$, $m$, and $B$.

The scaling of $Z(\phi_p)$ is related to the scaling of the tube step length $a(\phi_p)$. This scales as $\phi_p^x$, where various arguments set $x$ as either $-1/2$ or $-1$ in concentrated solutions.[5] The experimental data appear closer to $-1/2$. The relationship $Za^2 = Nb^2$, which arises from the equality of the mean squared end-to-end distance of the primitive path and of the original chain, indicates that a value of $m = 1$ corresponds to $x = -1/2$. In semidilute solutions, the scaling depends somewhat on the quality of the solvent. A value of $x = -5/8$ corresponds[2,5] to a theoretical scaling of the plateau modulus as $\phi_p^{2.25}$. If we assume the mean squared end-to-end distance of the primitive path obeys the same excluded volume scaling as the original chain, we obtain $Z^{2\nu}a^2 = N^{2\nu}b^2$ by equating the squared end-to-end distance for the primitive path and the actual chain. Using $\nu = 3/5$, we obtain the scaling $Z \sim a^{-1/\nu} \sim \phi_p^{25/24}$. Experimental data suggest a somewhat higher exponent for the scaling of the plateau modulus in semidilute solutions. This results in a more negative value of $x$ and a somewhat higher power for the scaling of $Z$. In all cases, $Z$ is expected to scale approximately with an exponent of $m = 1$ or a little larger.

In Figure 1a, $m$ has a value of 8.0, which is probably unrealistically large. However, we include this example because it provides a clear illustration of a certain behavior for the chemical potential. This value of $m$ causes the number of primitive path segments to decline rapidly as the $\phi_p$ decreases. As a result the maximum in the $\mu_s^{OR}$ occurs for a fairly concentrated solution. In this case the maximum in $\mu_s^{OR}$ produces a local maximum in the total solvent chemical potential $\mu_s$. For values of $\mu_s$ between its value at the local maximum, $\mu_s^{max}$, and its value at the local minimum, $\mu_s^{min}$, there are three corresponding values of $\phi_p$. It is not difficult to demonstrate that when this occurs, there is a unique pair of values $\phi_{pA}$ and $\phi_{pB}$ for which the conditions

$$\mu_s(\phi_{pA}) = \mu_s(\phi_{pB}) \tag{13}$$

and

$$\mu_p(\phi_{pA}) = \mu_p(\phi_{pB}) \tag{14}$$

are both satisfied. This is discussed in Appendix B. The smaller of these values for $\phi_p$, which we take to be $\phi_{pA}$, is less than the value of $\phi_p$ corresponding to the local minimum in $\mu_s$, while the larger of these, $\phi_{pB}$, is greater than the value of $\phi_p$ corresponding to the local maximum in $\mu_s$. Equations 13 and 14 are the conditions for phase separation, and the system forms two solution phases. The higher concentration solution has a polymer volume fraction of $\phi_{pB}$ at the boundary between the two solutions, and the more dilute solution has a polymer volume fraction of $\phi_{pA}$ at this boundary.

It is reasonable to assume that the solvent can only penetrate the pure polymer rather slowly. Therefore, at early times there is a region of essentially pure polymer into which little solvent has penetrated, there is a concentrated polymer solution phase, and there is dilute polymer solution phase. The polymer volume fraction at the interphase between the concentrated and dilute solutions is $\phi_{PA}$ for the dilute solution and $\phi_{pB}$ for the concentrated solution. The pure polymer region is not a distinct phase. Its presence at an early time reflects the slow diffusion of the solvent through the concentrated polymer solution. In section III we present model calculations that illustrate this behavior. The sharpness of the boundary between the pure polymer region and the concentrated solution is likely to depend on the nature of the pure polymer, in particular whether it is glassy or a melt. This is discussed further in section III. As time progresses, two processes occur. The solvent penetrates further into the polymer, reducing the size of the nearly pure polymer region, and the stress due the orientational nonrandomness of the polymer segments relaxes. As the stress relaxes, the local maximum and minimum in the $\mu_s$ grow together. As this happens, $\phi_{pA}$ and $\phi_{pB}$ approach each other. Eventually the local maximum and minimum merge, the phase boundary disappears, and there remains only a single solution phase.

A smaller and more realistic value of $m = 1.0$ is chosen for $Z(\phi_p)$ in Figure 1b. Although it is not visible in the figure, there still is a small local minimum in $\mu_s^{OR}$ at small $\phi_p$. For small $\phi_p$, $\mu_s^{OR}$ has the asymptotic form $-(V_sK_BT/V_p)Z_1Nm\phi_p^{m+1} \ln \phi_p$ and $\mu_p^{OP}$ has the asymptotic form $-(V_sK_BT/V_p)\phi_p$. For all $m > 0$, $\mu_s^{OR}$ approaches zero faster than $\mu_s^{OP}$ as $\phi_p \to 0$ and $\mu_s$ must be negative for small $\phi_p$. For the values of the parameters of the model employed in Figure 1b, the system forms two solution phases.

However, the polymer volume fraction in the dilute solution is very small. The value of $\mu_s$ at the boundary must be very close to zero, and the polymer volume fraction for the concentrated solution at the boundary is very close to the largest value of $\phi_p$ at which $\mu_s$ crosses zero.

The polymer/solvent system in this case forms a concentrated solution and a dilute solution. At early times there is also a region of essentially pure polymer, just like the system corresponding to the $\mu_s$ shown in Figure 1a. Just as in that case, the size of the pure polymer region slowly decreases and the orientation stress relaxes as time progresses. The main difference between the two cases is that the polymer concentration in the dilute solution is very low. As the stress relaxes, this concentration remains small and the polymer volume fraction of the concentrated solution at the phase boundary decreases until eventually it reaches the value for the dilute solution and the boundary vanishes.

The relative importance of the orientational stress and osmotic pressure contributions to the chemical potential is determined by the relative magnitude of the parameters $Z_1$, which is $Z/N$ for the pure polymer, and $B$, which is related to $a_{OP}$ by (12). Large $Z_1$ and small $B$ favor the formation of a gel-like concentrated solution phase. In Figure 1c these parameters are chosen such that $\mu_s^{OR}$ is less significant compared with $\mu_s^{OP}$ than in the cases shown in Figure 1a,b. As a result there is no local maximum in $\mu_s$, which is a monotonically decreasing function of $\phi_p$. In this case there is only a single solution phase. Figure 1c would also describe the chemical potential of a system, which originally supported two solution phases, at sufficiently long times that there has been significant relaxation of the orientational stress and the phase boundary between the solution phases has disappeared.

In obtaining the curves in Figure 1, we have used the form (10) for $\mu_s^{OP}$. As we pointed out, this form is reasonable for the dilute and semidilute regimes but does not decrease fast enough for larger $\phi_p$. This reflects the fact that the renormalization model employed in obtaining the osmotic pressure[4] used in (10) assumes the chains occupy zero volume. The important qualitative feature of $\mu_s^{OP}$ at larger values of $\phi_p$ is that it dominantes $\mu_s^{OR}$, which is true for this model and for a more accurate model. A more accurate model would result in some quantitative change in $\mu_s$, but the qualitative behavior that produces the two solution phases would remain the same.

**B. Stress Relaxation.** In the next section, we present simple numerical model calculations for the polymer/solvent system under the assumption that stress relaxation is slow. The choice of this limit is motivated by the fact that a precise calculation including stress relaxations requires a model for the concentration dependence of the reptation disengagement time $\tau_d$ which suffices for dilute through concentrated solutions. In general, such a model is not available. In this section we briefly discuss the relaxation within the reptation model, leaving open the question of the $\phi_p$ dependence of this disengagement time. We suggest some approximations that produce numerically tractable equations for the time dependence of the polymer volume fraction at the boundary between the concentrated and dilute solutions. From these equations this time-dependent $\phi_p$ can be evaluated, as well as the time at which the two phases merge into a single solution phase, once a model for $\tau_d(\phi_p)$ is specified.

In the reptation model the stress relaxes by means of diffusion of the polymer past the ends of the tube. First consider the simple case where the swelling occurs rapidly. Recall we are treating the average contour length $L$ as fixed. After the swelling each tube segment has a nonrandom distribution of orientations given by (A6). The primitive chain, which represents the polymer in the tube, evolves by Rouse dynamics.[2] An end of this chain takes a random distribution of orientations as it diffuses out of the tube enclosing the polymer after the swelling. In this way the moving chain ends create new tube segments that are randomly oriented. At a time $t$ later, the fraction of the segments in the original tube have the nonrandom distribution of orientations associated with the swelling, and these contribute to the stress. The other segments that are no longer in the original tube do not contribute to the stress.[2] Therefore, to calculate the stress at time $t$, we merely need to multiply the original stress by the fraction of the chain segments still in the original tube. This factor has been calculated by Doi and Edwards[2] as

$$\psi(t) = \sum_{j=1,3,5,\ldots} \frac{8}{j^2\pi^2} \exp[-j^2 t/\tau_d] \tag{15}$$

where the disentanglement time is

$$\tau_d = \frac{L^2}{\pi^2 D_R} \tag{16}$$

and $D_R$ is the Rouse diffusion constant for the center of mass motion of the chain. $\tau_d$ scales as $N^3$, where $N$ is the number of monomers in the polymer, and $\tau_d$ depends on $\phi_p$ through $L$ and possibly through $D_R$. We can summarize this by writing

$$\tau_d = \tau_{d1} f_\tau(\phi_p) \tag{17}$$

where $\tau_{d1} = \tau_d(\phi_p = 1)$.

In general, the swelling and stress relaxation occur simultaneously. In this case, the orientational stress contribution to the free energy per unit volume at time $t$ can be written

$$\overline{\Delta G}^{OR} = \frac{Z(\phi_p)\phi_p}{V_p}[\Delta G_{seg}^{OR}(\Phi(t,0))\Psi(t,0) + \int^t dt_1\, \Delta G_{seg}^{OR}(\Phi(t,t_1))\rho(t,t_1)] \tag{18}$$

where the solvent is added to the polymer at $t = 0$ and we have defined $\Phi(t,t_1) = \phi_p(t)/\phi_p(t_1)$ and $\phi_p$ denotes $\phi_p(t)$ in (18). The function $\Psi(t,t_0)$ is the generalization of $\psi(t)$ of eq 15 to allow for the time dependence of $\tau_d(\phi_p)$

$$\Psi(t,t) = \sum_{j=1,3,5,\ldots} \frac{8}{j^2\pi^2} \exp\left\{-\frac{j^2}{\tau_{d1}} \int_{t_1}^{t} f_\tau^{-1}[\phi_p(t_2)]\, dt_2\right\} \tag{19}$$

$\Psi(t,0)$ is the fraction of the chain that occupies tube that was part of the original tube at $t = 0$. This is the fraction of the tube at $t$ that has not been visited by either chain end between $t = 0$ and $t$. The function $\rho(t,t_1)$ is the distribution of times $t_1$ at which a given tube segment occupied by chain at time $t$ was last visited by a chain end, averaged over all chain segments. If the tube was last visited by a chain end at $t_1$, then its distribution of orientations was randomized then, but not since. Thus, the swelling of the polymer network between $t_1$ and $t$ results in a nonrandom distribution of orientations and a stress contribution to the free energy given by the second term in (18). The distribution of last randomization times, $\rho(t,t_1)$, and the probability density for no randomization between $t_1$ and $t$, $\Psi(t,t_1)$, are related by[2]

$$\rho(t,t_1) = \frac{\partial}{\partial t_1}\Psi(t,t_1) \tag{20}$$

Substitution of (17) into (3) and (4) gives

$$\mu_s^{OR}(t) = \Psi(t,0)\tilde{\mu}_s^{OR}(t,0) + \int_0^t \tilde{\mu}_s^{OR}(t,t_1)\rho(t,t_1)\,dt_1 \quad (21)$$

$$\mu_p^{OR}(t) = \Psi(t,0)\tilde{\mu}_p^{OR}(t,0) + \int_0^t \tilde{\mu}_p^{OR}(t,t_1)\rho(t,t_1)\,dt_1 \quad (22)$$

where the chemical potentials with tildes on the right-hand side of (21) and (22) are the values obtained with $\Delta\tilde{G}^{OR}$ from (8), which assumes no stress relaxation between $t_1$ and $t$.

$\Psi(t,t_1)$ and $\rho(t,t_1)$ involve the time integral of $\tau_d^{-1}$ between $t_1$ and $t$. This integral is evaluated by using the function $\phi_p(t)$ appropriate for a specific location in the polymer/solvent system, i.e., a specific tube segment. As the entangled polymer swells, this point moves in space along with the chains. This function $\phi_p(t)$ varies with the point in the system, although we have suppressed this positional dependence for notational simplicity.

In principle, (21) and (22) can be employed together with the osmotic pressure contributions to $\mu_s$ and $\mu_p$ to obtain appropriate equations for solvent and polymer diffusion in the system. This results in a partial differential equation for the function $\phi_p(x,t)$. However, a detailed calculation of $\phi_p(x,t)$ from this equation would be very cumbersome, if not impractical, since it would require storing the entire history of $\phi_p$ for each $x$ and for all times from zero to $t$ as well as performing the $\int f_\tau^{-1}\,dt$ integral in the functions $\Psi$ and $\rho$ and the $\int \rho\tilde{G}\,dt$ integral in $\mu_s^{OR}$ and $\mu_p^{OR}$. Therefore, rather than attempt to numerically solve this partial differential equation, we focus on the stress relaxation at the boundary between the concentrated and dilute solution phases.

The evaluation of the polymer volume fraction at the boundary between the concentrated solution and the dilute solution is greatly simplified by assuming the first term in (21) and (22) dominates and neglecting the second term in each equation. This approximation should be reasonable when the unrelaxed solvent chemical potential displays the behavior shown in Figure 1b. When the polymer and solvent are brought into contact, there is a rapid dilution and swelling of the polymer as the concentrated solution and the phase boundary is established. The stress associated with this swelling relaxes as the polymer chain ends reptate out of the original tube. This relaxation results in an additional slow swelling of the entangled polymer system. This subsequent swelling increases the $\mu_s^{OR}$ contribution from the unrelaxed chain segments and causes the relaxed segments to assume a nonrandom distribution of orientations. This latter effect is accounted for by the second term in (21) and (22). However, since the polymer solution is already partially diluted at the time of the initial relaxation of the chain segment, the contribution to the chemical potential from these already relaxed segments is not that great. (Recall that the contribution to the free energy per segment at time $t$ depends on the ratio of $\phi_p$ at the time of last relaxation by reptation and $\phi_p$ at $t$.) Furthermore, the stress relaxation at early times occurs predominantly near the chain ends. As these relaxed chain segments begin to develop additional stress due to the subsequent dilution and swelling, they tend to be relaxed again by the reptation of the chain.

In the case shown in Figure 1b the polymer volume fraction in the dilute phase is very small, and we can assume the stress contribution is negligible for this phase. The value of $\phi_p$ for the concentrated solution at the boundary is well approximated by the largest value for which $\mu_s$ is zero. The corresponding condition for the disappearance of the distinct phase boundary is that the local maximum in $\mu_s$ has the value $\mu_s = 0$. Any additional stress relaxation results in a functional form of $\mu_s$ that never crosses zero for $\phi_p > 0$. This condition is, of course, an approximation to the exact condition that the two solution phases merge when the local maximum and minimum in $\mu_s$ merge. However, the evaluation of $\phi_p$ at the boundary from the $\mu_s = 0$ condition results in considerable numerical simplification since it only involves a single condition on $\mu_s$, rather than the simultaneous conditions on $\mu_s$ and $\mu_p$ given by (13) and (14). In either case, the evaluation of $\phi_p(t)$ at the boundary and $\Psi(t,0)$ requires models for the concentration dependence of $\tau_d$ and $Z$. These calculations involve the range of polymer concentrations from concentrated solutions to semidilute to dilute solutions, and at present accurate models for $\tau_d$ spanning this the entire range are, unfortunately, not available.

## III. Simple Model Calculations

In this section we present simple model calculations in order to illustrate the possible behavior of the systems for the case when the chemical potential versus polymer volume fraction plot resembles Figure 1b. In this case there is a phase separation into concentrated and dilute solutions, and the polymer volume fraction in the dilute solution is quite low. For simplicity we assume a one-dimensional geometry, which corresponds, for instance, to the case of solvent added on top of a layer of pure polymer. We model the solvent volume fraction $\phi_s$ as obeying a diffusion equation in concentrated solution region.

$$\frac{\partial\phi_s}{\partial t} = \frac{\partial}{\partial x}\left[D\frac{\partial\phi_s}{\partial x}\right] \quad (23)$$

The diffusion coefficient in (23) is called the mutual diffusion coefficient.[6] In a two-component system such as this, there is in general a bulk flow term for a given component that arises in response to the diffusive flux of the other component. Recall we are assuming no change in the molecular volumes $V_p$ and $V_s$ on mixing. In a closed stationary system, if one component diffuses in one direction, there must be a compensating flux of the other component in the opposite direction. However, the diffusive and bulk flow flux terms can be combined to give the simple diffusion form,[6] e.g., (23). The mutual diffusion constant contains contributions from the solvent and polymer diffusion coefficient. However, we can safely assume that the polymer diffusion coefficient is very small compared to the solvent coefficient, and $D$ is essentially the concentration-dependent solvent diffusion coefficient. It is generally a decreasing function of polymer volume fraction.

Since $\phi_p = 1 - \phi_s$, the polymer volume fraction obeys a similar diffusion equation

$$\frac{\partial\phi_p}{\partial t} = \frac{\partial}{\partial x}\left[D\frac{\partial\phi_p}{\partial x}\right] \quad (24)$$

Notice $D$ is the same diffusion coefficient as in (23). This is because the polymer flux is mainly a bulk flow flux in response to the diffusive solvent flux.

The diffusion coefficient can be expressed in terms of the thermodynamic forces, $-\partial\mu_s/\partial\phi_p$ and $-\partial\mu_p/\partial\phi_p$, and the appropriate concentration-dependent mobility coefficients. However, since these model calculations are intended only to illustrate the expected behavior of the system, we merely model $D$ as a simple exponential

$$D = D_0 \exp[a_D(1 - \phi_p)] \quad (25)$$

This form has been used elsewhere in the literature[7] to model polymer concentration dependence of the solvent

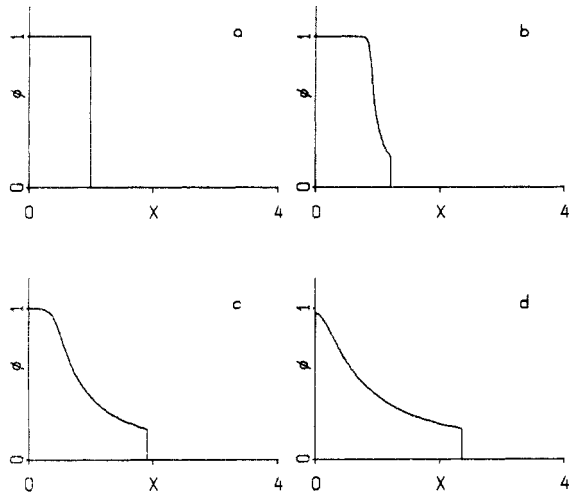


**Figure 2.** Polymer volume fraction profiles as a function of dimensionless position at various times. The model parameters are $a_D = 5$ and $\phi_{pb} = 0.2$. The dimensionless times are $t = 6.74 \times 10^{-4}$ for case a, $t = 3.37 \times 10^{-3}$ for case b, $t = 1.35 \times 10^{-2}$ for case c, and $t = 3.03 \times 10^{-2}$ for case d.

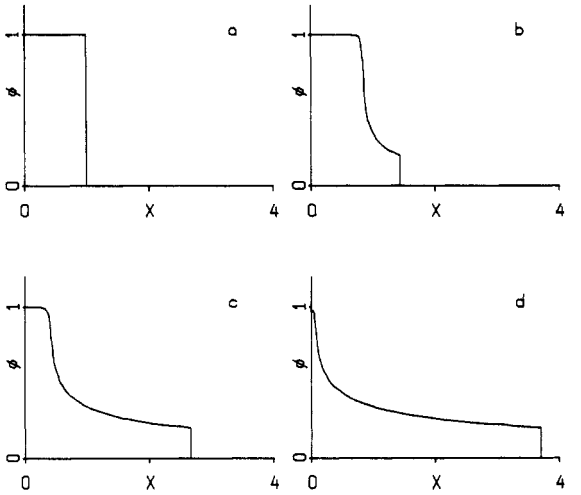


**Figure 3.** Polymer volume fraction profiles as a function of dimensionless position at various times. The model parameters are $a_D = 10$ and $\phi_{pb} = 0.2$. The dimensionless times are $t = 9.08 \times 10^{-5}$ for case a, $t = 4.54 \times 10^{-4}$ for case b, $t = 1.36 \times 10^{-3}$ for case c, and $t = 3.63 \times 10^{-3}$ for case d.

diffusion coefficient, and it has the main features we desire: it is a smoothly and rapidly decaying function of polymer concentration.

For the sake of simplicity we assume that the polymer volume fraction in the dilute solution phase is quite low. If this low concentration is established throughout this phase quite rapidly compared with the time scale of the swelling of the concentrated polymer phase, then we can treat the polymer flux across the boundary between the dilute and concentrated phases as negligible. Since the gel-like concentrated polymer solution is swelling, the boundary between this phase and the nearly pure solvent phase, $x_b$, is moving with velocity $\dot{x}_b$. This boundary velocity can be evaluated from the flux at $x_b$

$$\left[-D\frac{\partial \phi_p}{\partial x}\right]_{x_b} = \dot{x}_b \phi_{pb} \tag{26}$$

The left side is the polymer flux evaluated at $x_b$, and $\phi_{pb}$ is the polymer volume fraction for the concentrated solution at the boundary $x_b$. In time $\delta t$ the boundary moves from $x_b$ to $x_b + \dot{x}_b \delta t$ and the amount of polymer per surface area between $x_b$ and $x_b + \dot{x}_b \delta t$ is $\phi_{pb}\dot{x}_b \delta t$ to first order in $\delta t$. The flux at $x = x_b$ is obtained by dividing this by $\delta t$, which yields (26). In addition to (26), there is also the condition that $\phi_p(x_b) = \phi_{pb}$ is constant at this moving boundary. Equation 24, together with this boundary condition at $x_b$, the boundary condition $J_p = 0$ at $x = 0$, and the expression for $\dot{x}_b$, (26), defines our simple model.

The parameters in this simple model are the polymer volume fraction of the concentrated phase at the phase boundary, $\phi_{pb}$, the initial width of the slab of pure polymer to be dissolved, $w$, and the two parameters that define the concentration-dependent diffusion constant, the $D_0$ and $a_D$ of eq 25. Of these, $\phi_{pb}$ an $a_D$ are dimensionless, and the combination $w^2/D_0$ has units of time. If we recast the diffusion equation (24) in terms of the dimensionless length $y = x/w$ and dimensionless time $\tau = D_0 t/w^2$, it takes the form

$$\frac{\partial \phi_p}{\partial \tau} = \frac{\partial}{\partial y}\left[ d(\phi_p)\frac{\partial \phi_p}{\partial y}\right] \tag{27}$$

where $d(\phi_p) = D(\phi_p)/D_0$. The resulting polymer concentration profile $\phi_p(y,\tau)$ depends on the two model parameters $\phi_{pb}$ and $a_D$.

Figure 2 shows $\phi_p(y,\tau)$ at various values of $\tau$ for $\phi_{pb} = 0.2$ and $a_D = 5$. At early times the polymer volume fraction rises steeply as a function of distance from the phase boundary until it smoothly approaches the essentially pure polymer limit. At these early times there is still quite an extensive region of polymer into which a negligible amount of solvent has penetrated. At later times this region of virtually pure polymer diminishes and the polymer volume fraction profile becomes less steep. This results in a lower polymer flux across this region. Since $J_s = -J_p$, the solvent flux necessary slows with time as well, and this is reflected in a slowing of the rate of solvent influx into the concentrated solution phase from the dilute, almost pure solvent phase.

At longer times the $\phi_p$ profile approaches a constant of $\phi_p(y,\tau) = \phi_{pb}$. This is not a true phase equilibrium since the orientational stress due to the swelling eventually relaxes. As this happens, $\phi_{pb}$ decreases, and eventually the phase boundary disappears.

If we vary the parameter $a_D$, it is evident from (25) that increasing $a_D$ increases the diffusion constant except at $\phi_p = 1$, where there is no effect. This results in an increase in the rate of solvent influx into the concentrated polymer region. The polymer volume fraction profiles tend to be flatter near the boundary with the dilute phase due to the increased diffusion constant for this region and steeper as the pure polymer region is approached due to the increased flux. The case with $a_D = 10$ is shown in Figure 3. If we increase the parameter $\phi_{pb}$ in the model, this has the general effect of slowing the swelling rate, due to a general reduction in the steepness of $\phi_p$ profile.

These simple model calculations are intended to illustrate the expected behavior of these systems for the case where the stress relaxation is very slow compared with the swelling of the concentrated polymer region. This assumes, of course, that the orientational stress term in the free energy is sufficiently large compared with the osmotic term, so as to support a phase boundary for times short compared with the stress relaxation time.

We have assumed throughout that the contour length of the primitive paths associated with the polymer chains relaxes on a time scale short compared with the swelling time. This contour length relaxation takes place on the scale of the Rouse time, $\tau_R$, which varies with degree of polymerization as $N^2$. The time scale for stress relaxation is the reptation disengagement time $\tau_d$, which varies as $N^3$. Thus, there are many orders of magnitude between

these time scales. On the other hand, the diffusion constant in the model is essentially the diffusion constant for the diffusion of the solvent in the concentrated polymer. It has little or no dependence of $N$. As a result, the swelling time scale in the model has essentially no $N$ dependence. Thus, a given polymer/solvent system may obey the time scale assumptions of this simple model for some range of $N$, but not for others. As $N$ becomes too small, the stress relaxation time scale must become compariable to the swelling time scale. In the limit of very large $N$, the neglect of contour length relaxation should no longer be valid, and there should be an additional elastic contribution to the free energy and chemical potentials due to contour length variations.

If the pure polymer is glassy, then the contour relaxation time may be slow for the glassy region where almost no solvent has penetrated, and it may still be very fast compared with the swelling time scale in those regions of the concentrated solution phase where there is sufficient penetrant so that the system is no longer glassy. This could lead to behavior like that observed in the absorption of a solvent into an initially glassy pure cross-linked polymer.[7-9] In this case a sharp front is observed between the nearly pure polymer region and the region of the concentrated solution into which the penetrant has been extensively absorbed. This front behavior is in contrast to the behavior displayed in Figures 2 and 3, where the polymer volume fraction smoothly approaches the pure polymer limit. In the case with the front behavior, the front commonly advances with a nearly constant velocity until the essentially pure polymer region vanishes. This behavior, which is called type II diffusion, has been modeled[7-9] by assuming that there is a back pressure to penetrant influx that opposes the osmotic pressure. This back pressure is the result of the stretching of the polymer contours in the current picture. The additional back pressure has been treated[7,9] as proportional to the local rate of swelling, $P = \eta(d\phi_s/dt)$, where the proportionality constant $\eta$ is taken to be the elongation viscosity. The elongation viscosity is assumed to decrease rapidly as $\phi_s$ increases, so that this contribution to the chemical potential falls off rapidly away from the pure polymer limit.

If a system were to exhibit this type of behavior during dissolution, it would display three regions, separated by sharp boundaries, a nearly pure polymer region, a concentrated solution region, and a dilute solution, nearly pure solvent, region. In this case the boundary between the nearly pure polymer and the concentrated solution would move with nearly constant velocity so as to reduce the size of the nearly pure polymer region.

## IV. Discussion

We have presented a model for the dissolution of a bulk polymer into a solvent based upon reptation dynamics. The chemical potentials of the solvent and polymer are examined. Two contributions are included in these chemical potentials. The first is the normal contribution due to mixing, which is equal to $-V_s\Pi(\phi_p)$. The second contribution arises from the swelling of the entangled polymer due to the influx of the solvent. This results in a nonrandom distribution of orientations for the polymer segments, which produces an orientational contribution to the free energy. We evaluate the orientational contribution to the free energy and to $\mu_s$ and $\mu_p$ using the concept of the primitive chain from reptation theory.

The first contribution depends on the osmotic pressure and the second term involves the number segments in the primitive chain, both of which are functions of polymer volume fraction. While mathematical models are not available for these functions, which are accurate over the entire range of polymer concentration, their qualitative behaviors are understood. If the orientational contribution $\mu_s$ is sufficiently large compared with the osmotic contribution, then the polymer/solvent system segregates into a concentrated, gel-like solution phase and a dilute solution phase. An analysis of the renormalization group results[4] for the osmotic pressure of a polymer/solvent system in the semidilute regime under good-solvent conditions indicates the magnitude of the osmotic contribution to $\mu_s$ is influenced by the factor $B = b^3/V_m$, where $b$ is approximately the Kuhn length and $V_m$ is the average volume per monomer. Under semidilute, good-solvent conditions $\mu_s^{OP} \sim B^{5/4}$. In general, $\mu_s^{OP}$ is also affected by solvent quality. For larger $\phi_p$, deviations from the renormalization group semidilute result for $\mu_s^{OP}$ become important. Nevertheless, the semidilute result should provide a reasonable qualitative guide for the expected behavior of a given polymer/solvent system.

The orientational contribution to $\mu_s$ contains two terms. One is proportional to $Z(\phi_p)$ and the other is proportional to $dZ/d\phi_p$. Thus, it is the number of primitive path segments that determines the magnitude of this contribution to $\mu_s$. Large $Z$ and small $B$ favor segregation into two distinct polymer/solvent solution phases.

The nonrandom distribution of orientations of the polymer chain segments relaxes with time toward a random distribution. This can be treated within the reptation model.[2] At a sufficiently long time, the orientational contribution to $\mu_s$ is sufficiently reduced by this relaxation, and the distinct phase boundary between the two solution phases, if present initially, disappears, leaving a single soltuion phase. We have discussed the general treatment of the stress relaxation, as well as some simplifying assumptions that should be reasonable for this problem. A calculation of the relaxation and the time for the disappearance of the phase boundary requires a detailed knowledge of the concentration dependence of the reptation disengagement time $\tau_d$. This is generally not available. However, it is evident that the relaxation time grows with $\tau_d$ and it is known that this function scales with degree of polymerization as $N^3$. For the concentrated solutions it is also inversely proportional to the square of the segment length for the primitive chain.

Simple numerical calculations have been presented to illustrate the expected behavior of polymer/solvent systems for which the orientational stress contribution to the free energy is sufficiently large to support a phase separation into a concentrated gel-like solution phase and a dilute, nearly pure solvent phase. A mutual diffusion coefficient that is an exponentially decreasing function of $\phi_p$ is employed, and it is assumed that the polymer flux across the boundary between the concentrated solution region and the nearly pure solvent region is negligible. In this case the calculations display a nearly pure polymer region. This region is not separated from the concentrated solution phase by a distinct boundary and is merely a region into which significant solvent has not yet reached. The size of this region decreases with time and eventually it disappears. The calculations also show that the rate of swelling and solvent influx diminishes with time.

**Acknowledgment.** This work is supported by NSF Grant CHE85-14823 to M.F.H.

## Appendix A

In this appendix we evaluate the distribution of orientations of a chain segment induced by the swelling

of the network which accompanies the influx of solvent. The initial distribution of orientations for the chain segment is taken to be random. The $z$ direction is arbitrarily chosen to be the direction of swelling. As the polymer volume fraction decreases from an initial value of $\phi_{p0}$ to a value of $\phi_{p1}$, a small volume element containing a portion of the polymer network swells from $V_0$ to $V_1 = V_0\phi_{p0}/\phi_{p1}$ to accommodate the influx of solvent. Since the swelling occurs along the $z$ direction, a small displacement in this direction $\Delta z_0$ at $t_0$ swells to $\Delta z_1$ at $t_1$. This dilation of the network in the $z$ direction is given by

$$\Delta z_1/\Delta z_0 = \phi_{p0}/\phi_{p1} \equiv \Phi^{-1} \tag{A1}$$

If a chain segment is originally oriented in the direction specified by the unit vector $\hat{u}_0$, then after the swelling it is oriented in the direction of the unit vector

$$\hat{u} = \frac{\hat{e}_x u_{x0} + \hat{e}_y u_{y0} + \hat{e}_z u_{z0}\Phi^{-1}}{\sqrt{u_{x0}^2 + u_{y0}^2 + \Phi^{-2}u_{z0}^2}} = \frac{\hat{e}_x \sin\theta_0 \cos\phi_0 + \hat{e}_y \sin\theta_0 \sin\phi_0 + \hat{e}_z\Phi^{-1}\cos\theta_0}{\sqrt{1 + (\Phi^{-2} - 1)\cos^2\theta_0}} \tag{A2}$$

Equation A2 involves the assumption that the polymer network undergoes an affine deformation. It also ignores the fact that the chain length relaxes in the tube as the network swells. It is the tube that reorients. The position of a primitive chain segment in the tube changes as the tube length varies under the affine deformation, since the chain length does not vary along with the tube length. The reoriented vector $\hat{u}$ should be obtained by (A2) from a $\hat{u}_0$ associated with the earlier time orientation of some other point along the primitive path. Ignoring this repositioning of the chain segment in the tube during the deformation is the well-known independent alignment approximation.[2]

The distribution of $\xi = \cos\theta$ is obtained from (A2) by identifying the coefficient of $\hat{e}_z$ as $\cos\theta$. Therefore

$$f(\xi;\Phi) = \frac{1}{4\pi}\int_0^{2\pi} d\varphi_0 \int_{-1}^{+1} d\xi_0 \delta(\xi - \Phi^{-1}\xi_0/\sqrt{1 + \eta\xi_0^2}) \tag{A3}$$

where $\xi_0 = \cos\theta_0$, $\eta = \Phi^{-2} - 1$, and the distribution of initial orientations is taken to be uniform. Defining

$$\xi_1(\xi_0) = \Phi^{-1}\xi_0/\sqrt{1 + \eta\xi_0^2} \tag{A4}$$

we have

$$f(\xi;\Phi) = \frac{1}{2}\int_{-1}^{1} d\xi_0 \delta[\xi - \xi_1(\xi_0)] = \frac{1}{2}\int_{-1}^{1} d\xi_1 \left[\frac{d\xi_1}{d\xi_0}\right]^{-1} \delta(\xi - \xi_1) = \frac{1}{2}\left[\frac{d\xi_1}{d\xi_0}\right]^{-1}_{\xi_1=\xi} = \Phi^{-1}(1 + \eta\xi_0^2)^{-3/2} \tag{A5}$$

We need to invert (A4) to get $\xi_0$ as a function of $\xi_1$ and evaluate this at $\xi_1 = \xi$. This is accomplished by squaring both sides of (A4) and rearranging. Solving for $1 + \eta\xi_0^2$ and substituting into (A5) yield

$$f(\xi;\Phi) = \frac{1}{2}\Phi[1 - (1 - \Phi^2)\xi^2]^{-3/2} \tag{A6}$$

Equation A6 gives the distribution of $\xi = \cos\theta$ for an initially randomly oriented chain segment at a point in the polymer network which undergoes a swelling due a decrease in the $\phi_p$ from $\phi_{p0}$ to $\phi_{p1}$. Since the swelling is entirely along the $z$ direction, the distribution of the angle $\varphi$ remains uniform.

## Appendix B

In this appendix we show that whenever $\mu_s(\phi_p)$ has a local maximum and a local minimum, then there is a unique pair of values $\phi_{pA}$ and $\phi_{pB}$ satisfying the conditions for phase separation (13) and (14). From (3) and (4), it follows that

$$\mu_p = V_p\frac{\bar{G}}{\phi_p} - \frac{V_p}{V_s}\frac{1 - \phi_p}{\phi_p}\mu_s \tag{B1}$$

Now suppose $\phi_{pA}$ and $\phi_{pB}$ are chosen so that $\mu_s(\phi_{pA}) = \mu_s(\phi_{pB}) \equiv \mu_{s0}$. From (3) we also find

$$\frac{\bar{G}(\phi_{pB})}{\phi_{pB}} - \frac{\bar{G}(\phi_{pA})}{\phi_{pA}} = -V_s^{-1}\int_{\phi_{pA}}^{\phi_{pB}}\frac{\mu_s}{\phi_p^2}d\phi_p = V_s^{-1}\mu_{s0}\left[\frac{1}{\phi_{pB}} - \frac{1}{\phi_{pA}}\right] - V_s^{-1}\int_{\phi_{pA}}^{\phi_{pB}}\frac{\Delta\mu_s}{\phi_p^2}d\phi_p \tag{B2}$$

where $\Delta\mu_s = \mu_s(\phi_p) - \mu_{s0}$. Equation B1 shows that

$$\mu_p(\phi_{pB}) - \mu_p(\phi_{pA}) = V_p\left[\frac{\bar{G}(\phi_{pB})}{\phi_{pB}} - \frac{\bar{G}(\phi_{pA})}{\phi_{pA}}\right] - \mu_{s0}\frac{V_p}{V_s}\left[\frac{1}{\phi_{pB}} - \frac{1}{\phi_{pA}}\right] = -\frac{V_p}{V_s}\int_{\phi_{pA}}^{\phi_{pB}}\frac{\Delta\mu_s}{\phi_p^2}d\phi_p \tag{B3}$$

where the last equality follows from (B2).

Equation B3 demonstrates that condition (14) is satisfied if $\phi_{pA}$ and $\phi_{pB}$ are chosen so that the integral of $\Delta\mu_s/\phi_p^2$ from $\phi_{pA}$ to $\phi_{pB}$ is zero. There is one choice of $\mu_{s0}$ and, consequently, of $\phi_{pA}$ and $\phi_{pB}$ for which the value of this integral is zero. To see this, notice first that if $\mu_{s0}$ is set to the value of $\mu_s$ at the local minimum, $\mu_s^{min}$, then the integrand is everywhere positive, and so the integral must be positive. On the other hand, if $\mu_{s0}$ is set to $\mu_s^{max}$, the value at the local maximum, then the integrand is everywhere negative and the integral is less than zero. Let $\phi_p^{min}$ and $\phi_p^{max}$ be the values of $\phi_p$ corresponding to $\mu_s^{min}$ and $\mu_s^{max}$, respectively. As $\mu_{s0}$ is varied from $\mu_s^{min}$ to $\mu_s^{max}$, the integral monotonically decreases. Therefore, there is one and only one value of $\mu_{s0}$ for which the integral of $\Delta\mu_s/\phi_p^2$ vanishes. When performing this integral, we choose $\phi_{pA}$ to be less than or equal to $\phi_p^{min}$ and $\phi_{pB}$ to be greater than or equal to $\phi_p^{max}$.

This argument needs to be altered if $\mu_s^{max} > 0$, as in Figure 1b. In this case rather than setting $\mu_{s0} = \mu_s^{max}$ in the second step of the argument, we set $\mu_{s0} = 0$. We are assuming that there is a small local minimum in $\mu_s$ for small $\phi_p$ and that near $\phi_p = 0$ $\mu_s$ is dominated by the $-(V_sK_BT/V_p)\phi_p$ term from $\mu_s^{OP}$ as discussed in section II.A. Given this form, $\mu_s/\phi_p^2$ behaves as $-\phi_p^{-1}$ near the origin. The integral of $\mu_s/\phi_p^2$ from $\phi_p = 0$ to the largest value of $\phi_p$ at which $\mu_s = 0$ goes to $-\infty$, due to this $-\phi_p^{-1}$ singularity in the integrand at $\phi_p = 0$. Therefore, there must be a value of $\mu_{s0}$ between zero and $\mu_s^{min}$ for which the integral of $\mu_s/\phi_p^2$ vanishes. This integral is taken from the lowest value of $\phi_p$ to the largest value of $\phi_p$ satisfying $\mu_s(\phi_p) = \mu_{s0}$.

## References and Notes


(1) Brochard, F.; de Gennes, P.-G. *Physicochem. Hydrodyn.* **1983**, *4*, 313.
(2) Doi, M.; Edwards, S. F. *The Theory of Polymer Dynamics*; Clarendon Press: Oxford, 1986.
(3) de Gennes, P.-G. *Scaling Concepts in Polymer Physics*; Cornell University Press: Ithaca, NY, 1979.
(4) Cherayil, B. J.; Bawendi, M. G.; Miyake, A.; Freed, K. F. *Macromolecules* **1986**, *19*, 2770.
(5) Edwards, S. F. *Proc. R. Soc. London* **1988**, *A419*, 221.

(6) Crank, J. *The Mathematics of Diffusion*; Clarendon Press: Oxford, 1975.

(7) Thomas, N. L.; Windle, A. H. *Polymer* **1982**, *23*, 529.

(8) Hui, C.-Y.; Wu, K.-C.; Lasky, R. C.; Kramer, E. J. *J. Appl. Phys.* **1987**, *61*, 5129.

(9) Hui, C.-Y.; Wu, K.-C.; Lasky, R. C.; Kramer, E. J. *J. Appl. Phys.* **1987**, *61*, 5137.

# Comparative Calorimetric Study of Epoxy Cure by Microwave vs Thermal Energy

**Jovan Mijović* and Jony Wijaya**

*Chemical Engineering Department, Polytechnic University, 333 Jay Street, Brooklyn, New York 11201*

*Received December 18, 1989; Revised Manuscript Received February 13, 1990*

ABSTRACT: An investigation was carried out into the kinetics of cure of an epoxy formulation by microwave versus thermal energy. The formulation consisted of a diglycidyl ether of bisphenol A (DGEBA) type epoxy resin and diaminodiphenyl sulfone (DDS) curing agent. Differential scanning calorimetry (DSC) was used to measure and compare the degree of cure ($\alpha$) and the glass transition ($T_g$) of samples cured at the same temperature in microwave and thermal fields. A description of the microwave circuit is given. It was found that in the temperature interval used in this study (155–195 °C), cure proceeded slightly faster in thermal than in microwave field. Also, a broader glass transition range was observed in microwave-cured samples, suggesting a possible difference in the mechanism of cure in thermal and microwave fields.

## Introduction

Advanced fiber-reinforced polymer-matrix composites are nowadays extensively used as metal replacements in the production of commercial and military aerospace parts. In a recent announcement, the U.S. Government has designated the technology of advanced composites as one of the 22 technologies crucial to national security.[1]

The most widely used matrix materials for advanced composites are thermoset epoxy resins which are processed by cure, i.e., conversion of liquid monomers into a three-dimensional thermoset network via chemical reactions. During processing, heat is supplied to the sample by conduction and/or convection from a thermal energy source. Despite the prevalence of conventional thermal energy sources in the manufacturing of composites, their use results in long processing times and large temperature gradients in thicker samples.[2]

In the search for an alternative energy source for thermoset and composite cure, considerable interest has been generated in the application of electromagnetic waves in the microwave frequency range. A review of that topic has been recently published,[3] and examples of the use of microwave heating to cure polymers will not be restated here. Suffice it to say that, in contrast to thermal heating, which involves heat conduction and the thermal lag associated with it, microwaves can generate heat directly within the sample and thus offer possible advantages of higher efficiency, faster production rate, lower capital cost, more uniform cure, and improved physical/mechanical properties. Research efforts along those lines have been undertaken in several laboratories,[4-8] albeit no fundamental studies of the molecular interactions between the microwave field and polymers have been reported. Physical/mechanical properties of cured thermosets (and composites) depend on the thermoset network characteristics, and hence an understanding of the network formation during microwave cure is the first prerequisite in assessing the potential applicability of microwaves to composite processing.

## Objectives

Since microwave energy can be supplied directly to the sample, thus avoiding the conduction of heat through the processing equipment, it is clear that the overall processing time can be reduced by an appropriate process design. But the fundamental question that should be asked is whether cure reactions will proceed at different rates and by a different mechanism in microwave and thermal fields at the same temperature. For instance, in epoxy systems, where the kinetic mechanism can be quite complex,[9,10] could a preferential orientation of dipoles in the microwave field (as opposed to random orientation in the thermal field) alter the rates of individual reactions, leading to a different network morphology and properties? A comparative modeling study of kinetic mechanisms in thermal and microwave fields is in progress at the Polytechnic University and our initial results are reported here. The main objective of this paper is to directly compare the results of calorimetric measurements of rates of cure of an epoxy formulation at a series of isothermal conditions in thermal and microwave environments.

## Experimental Section

**Materials.** An epoxy formulation consisting of the stoichiometric amount of Shell's Epon 825 (diglycidyl ether of bisphenol A (DGEBA)) epoxy resin and diaminodiphenyl sulfone (DDS) was used in this study. The formulation was mixed and stirred for 10 min at 125 °C until a clear mixture was obtained. The mixture was either used immediately or stored in a freezer and used within 1 week.

**Processing.** Microwave cure was conducted in a microwave circuit assembled in our laboratory and shown in Figure 1.

* To whom correspondence should be addressed.

0024-9297/90/2223-3671$02.50/0 